Journal of Applied Polymer Science

Competitive adsorption of Ag (I) and Cu (II) by tripolyphosphate crosslinked chitosan beads

Chunxia Mao, Syed Ahmad Imtiaz, Yan Zhang
Department of Process Engineering, Faculty of Engineering & Applied Science, Memorial University of Newfoundland, St John's, NL A1B 3X5, Canada
Correspondence to: Y. Zhang (E-mail: yanz@mun.ca)

ABSTRACT: Alkalization of chitosan before crosslinking was applied in this study to enhance the adsorption capacity of the modified chitosan. Competitive adsorption of Ag (I) and Cu (II) from bimetallic solutions was studied using the newly synthesized tripolyphosphate crosslinked alkalized chitosan beads. Results indicated that alkalization before crosslinking helps to protect amine group from crosslinking and hence increases the uptake capacity and selectively of the synthesized beads toward Ag (I). The maximum uptakes of Ag (I) and Cu (II) were 82.9 and 15.5 mg g^{-1}, respectively, at room temperature with an initial concentration of each metal being 2.0 mM and the sorbent dosage of 1.0 g L^{-1}. The uptake of Ag (I) and Cu (II) by the beads can be better described by Langmuir isotherm and pseudo-second rate equation. Analyses from FTIR and XPS confirmed that free amine, hydroxyl, and $P_3O_{10}^{5-}$ groups are involved in metal binding with amine and hydroxyl groups more selective to Ag (I). © 2015 Wiley Periodicals, Inc. J. Appl. Polym. Sci. **2015**, *132*, 42717.

KEYWORDS: adsorption; crosslinking; ionic liquids; kinetics

Received 9 January 2015; accepted 10 July 2015
DOI: 10.1002/app.42717

INTRODUCTION

These years, biosorption has been considered as a promising technology for removal of heavy metals or recovery of precious metals from dilute solutions due to its low cost and high efficiency.[1] Chitosan produced from deacetylation of chitin, one of the most abundant polysaccharide next to cellulose, has been widely used as biosorbents to retain metal ions from aqueous solution.[2–6] Nevertheless, pure chitosan is easy to dissolve in acidic environments due to the presence of amine groups, limiting its applicability.[7] Chemical modifications of chitosan are thereby essential to improve its chemical stability, mechanical strength, and adsorption capacity in acidic media. The most common chemical modifications are crosslinking, grafting of new functional groups, and acetylation.[8]

Crosslinking of chitosan has been widely explored to enhance the chemical stability and mechanical strength of chitosan sorbents.[9] Four common crosslinking agents, glutaraldehyde, ethylene glycol diglycidyl ether (EGDE), tripolyphosphate (TPP) and epichlorohydrin (ECH), have been applied to immobilize chitosan powder. Because of the non-toxic nature and the low-cost, TPP is economically favorable for the synthesis of chitosan beads.[10] It is reported that the ionic reaction between chitosan and TPP was significantly influenced by the pH of TPP solution and the chitosan solution.[11] The degree of crosslinking of chitosan is higher in acidic environment; with the increase of pH, more OH^- will compete with $P_3O_{10}^{5-}$ and coagulate with chitosan, preserving more free $-NH_2$.[12] Several studies have been undertaken to synthesize TPP crosslinked chitosan beads for single metal adsorption.[9–13] However, very limited research works on the competitive adsorption of metallic ions with TPP crosslinked chitosan beads were reported.

Biosorption is a complex physicochemical process involving different sorption mechanisms. Understanding the adsorption mechanism is thus important because it enables the possibility for further improving the biosorption performance (e.g., capacity, selectivity, and adsorption rate). Although chemical reduction and precipitation have been incorporated into biosorption process by some researchers,[14–16] the sorption mechanism discussed in this study is only confined to physical adsorption. For passive physical sorption, mechanisms include electrostatic attraction, ion exchange, and chelation.[2] Electrostatic attraction arises when sorbent surfaces are charged with different signs of metal ions. Metal uptake through biosorption also takes place due to the ion exchange between the metal ions and protons on sorbent surfaces.[17,18] Chelation is based on coordination chemistry, in which one or more electron pairs of the ligand are donated to the metal to form complex ring-structure chelates. The most likely electron donor atoms are N,

O, and S in the forms of chemical groups of $-NH_2$, $=N-H$, $-OH$, $>C=O$, $-SH$, or $-OPO_3H$.[19]

The amine groups of chitosan play a key role in binding various metal ions, especially the transition metals.[2, 20, 21] It was reported that protonation of amine groups leads to ion exchange or electrostatic attraction mechanisms while the free electron doublet of nitrogen can explain the chelating properties of the polymer for metal cations in near neutral solutions.[2] For chemically modified chitosan sorbents, due to the introduction of grafted functional groups the sorption mechanisms of metal ions are more complex. Despite a large number of studies dedicated to the sorption of metal ions by modified chitosan, most of them focus on the evaluation of sorption performances and only a few of them aim at gaining a better understanding of sorption mechanisms. In addition, the majority of studies in biosorption area focused on the sorption of monometallic system; insufficient research has been carried out for the competitive adsorption from bimetallic or multi-metallic environment.

The primary objective of this study was to investigate the competitive adsorption of Ag (I) and Cu (II) on the TPP crosslinked alkalized chitosan (TCAC) beads. The purpose for studying the competitive sorption of Ag (I) and Cu (II) is twofold. First, copper and silver are from the same group in the periodic table. They have the same electron configurations in their valence shell and tend to have a shared chemistry.[22] It is therefore interesting to examine the competitive adsorption of these two metal ions. Second, silver and copper are very important industrial metals. Silver has been found to be widely distributed with low contents in copper ores.[23] Appreciable amounts of Ag (I) and Cu (II) coexist in wastewater from mining and mineral processing. Experimental study of the competitive biosorption of Ag (I) and Cu (II) can provide useful information for the recovery and separation of Ag (I) and Cu (II) from mining effluents. In the present work, effects of initial metal concentration and contacting time on the competitive adsorption of Ag (I) and Cu (II) were firstly studied. Different kinetics and isotherm models were then employed to describe the uptake of Ag (I) and Cu (II) on the prepared sorbent. The underlying sorption mechanisms of Ag (I) and Cu (II) were also clarified by comparing the FTIR and XPS results of sorbent before and after metal uptake. Finally, the desorption efficiency of Ag (I) and Cu (II) from the TCAC beads was assessed by using different eluents.

MATERIALS AND METHODS

Materials and Chemicals

Chitosan, copper, and silver nitrate standard solutions (100 m*M*) and 99.0% sodium tripolyphosphate (STPP) were purchased from Fisher (Canada). The average molecular weight and the deacetylation degree of chitosan are 100–300 kDa and 90.0%, respectively. A total of 99.0% sodium thiosulfate pentahydrate as well as ACS grade acetic acid, sulfuric acid, and ethylenediaminetetraacetic acid (EDTA) were purchased from Fisher also. Deionized (DI) water used for all experiments was generated from Milli-Q water purification system (Millipore Corporation) in the lab.

Preparation of TPP-crosslinked Chitosan Beads

Chitosan solution was prepared by dissolving 4.00 g chitosan powder in 100.0 mL of water containing 4.0% (v/v) acetic acid. The 5.0 and 10.0% (w/v) STPP solutions were prepared by dissolving 5.00 and 10.00g STPP powder in 100.0 mL of DI water, respectively. To synthesize TPP crosslinked alkalized chitosan (TCAC) beads, the chitosan solution was added dropwise into 250.0 mL of 0.5 M NaOH solution (pH = 8.6) using a syringe needle with inner diameter of 1.5 mm. The solidified beads were alkalized for 24.0 h prior to filtration and rinsed thoroughly with DI water. The alkalized chitosan beads were then immersed in 500.0 mL of 5.0 and 10.0% (w/v) STPP solutions (pH = 8.6) approximately 1.0 h for crosslinking. The formation of TCAC beads by the ionic reaction between phosphate groups of STPP and amino group of chitosan is schematically represented in Scheme 1. The beads were separated by filtration, washed four times with DI water and air dried before use. Dried TCAC beads were spherical and slightly yellowish in color. For comparison, the conventional TPP cross-linked chitosan (TCC) beads were also synthesized by adding the chitosan solution into the STPP solutions (pH = 8.6) directly, followed by filtration and a through rinsing with DI water. The TCC beads were air dried and sealed stored for use.

Swelling Rate Test

The swelling characteristics of TCAC beads was determined by immersing dried beads in 5.0 vol % HNO_3 solution, DI water, and 0.1 M NaOH solution and making the beads swell at 298.15 K for 24.0 h. After that, beads were removed from the swelling media and were blotted with a piece of paper towel to absorb excess water on surface. The swelling ratio of TCAC beads was calculated by the following equation:

$$E_{sw} = (W_s - W_d)/W_d \quad (1)$$

where E_{sw} is the percent swelling of beads in the equilibrium, W_s is the weight of swollen TCAC beads, and W_d is the weight of the dried TCAC beads.

Batch Sorption Tests

Bimetallic solutions containing equal moles of Ag (I) and Cu (II) ions were prepared from the standard 100.0 m*M* silver nitrate and copper nitrate solutions. As the initial pH of the equal molar bimetallic solutions is close to 5.0, batch sorption tests were conducted without adjusting the pH of the bimetallic solutions.

For sorbent screening, 100.0 mL monometallic and bimetallic solutions containing 1.0 m*M* $AgNO_3$ and/or 1.0 m*M* $Cu(NO_3)_2$ were equilibrated with 100.0 mg TCAC and TCC beads in 500 mL Erlenmeyer flasks shaking at 150 rpm for 24.0 h at 298.15 K. After filtration, the filtrate was analysed by ICP-OES to determine the final concentrations of metal ions in the solutions. The amount of adsorption, q_i (mg g^{-1}) for each metal ion [i = Ag (I) or Cu (II)] was calculated by:

$$q_i = \frac{(c_{i,0} - c_{i,e})V}{W} \quad (2)$$

where $c_{i,0}$ and $c_{i,e}$ (mg L^{-1}) are the initial and final concentrations of metal ion i in the solution; V (L) is the volume of bimetallic solution, and W (g) is the weight of the dry sorbent.

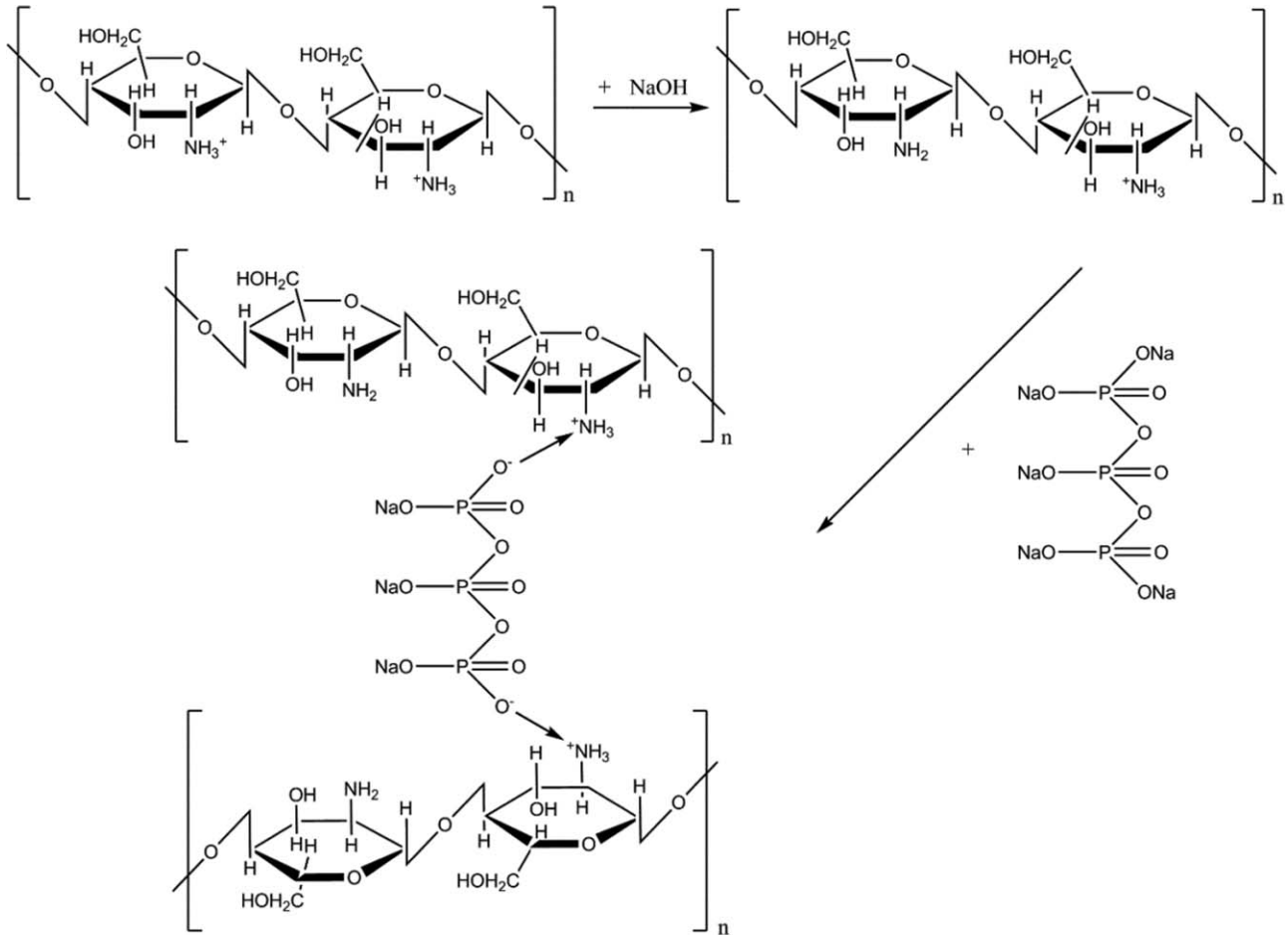

Scheme 1. Alkalization and crosslinking of chitosan with sodium tripolyphosphate.

Adsorption equilibrium study was carried out in an Innova® 43 console incubator shaker at 298.15 K. A total of 100.0 mL of bimetallic solutions with initial concentrations varying from 0.20 to 2.0 m*M* for each metal ion were fully mixed with 100.0 mg TCAC beads in 500.0 mL Erlenmeyer flasks, shaking at 150 rpm. After 48.0 h of equilibration, samples of 5.0 mL solution were withdrawn and filtered for later concentration measurement by ICP-OES.

Adsorption kinetics experiments were performed by the batch method at 300 K, where 300.0 mg of TCAC beads were suspended in 300.0 mL of Ag (I) and Cu (II) solution with 1.0 m*M* each metal ion in an Innova® 43 console incubator shakers at 150 rpm. Samples of 3.0 mL solution were taken at scheduled time interval and filtered for later concentration measurement by ICP-OES. The uptake of Ag (I) and Cu (II) at different sampling points can be calculated by eq. (3).

$$q_{i,j}=\frac{(c_{i,0}-c_{i,j})V-V_s\left(\sum_{k=1}^{j}c_{i,k}-jc_{i,j}\right)}{W} \quad (3)$$

where $q_{i,j}$ (mg g^{-1}) is the amount of metal ion i adsorbed at sampling point j ($j \geq 1$); $c_{i,j}$ (mg L^{-1}) is the concentration of metal ion i in the aqueous solution at sampling point j; k is an index referred to any sampling point till j ($k \leq j$); V and V_s (L) are the initial solution volume and the sampling volume, respectively; W (g) is the weight of the dry sorbent.

Desorption Tests

In general, adsorbed metal ions can be desorbed by acid, base, and chelating agents. In this study, dilute sulfuric acid, EDTA, and $Na_2S_2O_3$ solutions as well as their mixtures were used to regenerate the adsorbed TCAC beads. Desorption of Ag (I) and Cu (II) ions were carried out at room temperature with different eluents. A total of 100.0 mg of Ag (I) and Cu (II) loaded TCAC beads were immerged in 50.0 mL solutions; the initial pH of the solutions was adjusted using 1.0 M NaOH and 1.0 M H_2SO_4. The final concentration of metal ions in the aqueous phase was determined by atomic absorption spectrometer, and the pH variation of the solutions was determined by an accumet™ AB15 Basic and BioBasic™ pH/mV/°C Meter. The ratio of Ag (I) and Cu (II) desorbed from the saturated TCAC beads at time t, was calculated by:

$$\text{Des}\% = \frac{c_{i,e}V}{q_i W}\times 100\% \quad (4)$$

where Des % is the desorption ratio of Ag (I) and Cu (II) by desorption agents, q_i (mg g^{-1}) is the amount of copper or silver ion adsorbed on TCAC beads, $c_{i,e}$ (mg L^{-1}) is the measured concentration of copper or silver ion in the remaining liquid after desorption test, V (L) is the volume of the solution and W (g) is the mass of the TCAC beads.

Table I. Adsorption Studies[a] of Two Types of TPP-crosslinked Chitosan Beads from Monometallic and Bimetallic Solutions

No.	Alkalization	Crosslinking time (h)	Concentration of TPP (%)	Concentration of chitosan (%)	Capacity (mg/g)	
					Ag (I)	Cu (II)
1	NO	1.0	5.0	4.0	8.25	-
2	NO	1.0	5.0	4.0	-	16.50
3	YES	1.0	5.0	4.0	28.30	-
4	YES	1.0	5.0	4.0	-	8.90
5	NO	1.0	5.0	4.0	5.80	7.15
6	NO	1.0	10.0	4.0	6.65	7.94
7	Yes	1.0	5.0	4.0	31.54	3.89
8	Yes	1.0	10.0	4.0	32.28	4.84

[a] Batch sorption tests were carried out at $T = 25°C$ for 24.0 h.

ICP-OES

The concentrations of Ag (I) and Cu (II) ions in the solutions were measured by PerkinElmer® Optima™ 5300DV Inductively Coupled Plasma Optical Emission Spectrometer (ICP-OES) equipped with WinLab 32 for ICP v.4.0.0.0305 software. Sample solutions were diluted 20 times with 2.0% HNO_3 solution for the simultaneous measurement of all analytes. Standard solutions containing 0.0, 0.01, 0.1, 1.0, and 10.0 mg L^{-1} Ag (I) and Cu (II) in 2.0% HNO_3 were used to get the calibration curves. Yttrium (10.0 mg L^{-1}) was used as an internal standard to account for any difference between the sample matrix and calibration standards. Check standard solutions were prepared from PlasmaCal standards. Analysis on Ag was conducted at wavelengths of 338.290, 328.068, and 243.774 nm, analysis on Cu was performed at wavelengths of 327.393, 324.755, and 224.698 nm. Reported values were the mean of three consecutive replicate measurements and were corrected for dilution.

ATR–FTIR

The infrared spectra were recorded with a Bruker Alpha FTIR Spectrometer, using Single Bounce Diamond ATR accessory. The spectra were obtained with the average of 24 scans, at a 4 cm^{-1} spectral resolution. Peak identification was obtained from the corresponding second-derivative spectra in the range between 4000 and 400 cm^{-1}.

XPS

X-ray photoelectron spectra were performed on ULTRA spectrometer (Kratos Analytical) at the Alberta Centre for Surface Engineering and Science (ACSES), University of Alberta. Monochromatic Al *Kα* X-ray radiation was used as the excitation source (1486.6 eV) and operated at 144 W. Survey spectra were collected for binding energy spanning from 0 to 1100 eV with a pass energy of 80 eV and a step of 0.4eV. High resolution spectra for the C 1s, O 1s, N 1s, P 2p, Ag 3d, and Cu 2p regions were obtained, using pass energy of 40 eV with a step of 0.1 eV. The deconvolution of the high resolution spectra was made by XPSPEAK version 4.1, using the Gaussian/Lorentzian sum function.

SEM/EDS

The JEOL JSM-7100F (JOEL) scanning electron microscope (SEM) was used to examine the outer surface and cross-section of TCAC beads before and after metal adsorption. The Ag (I) and Cu (II) distribution on the cross-section of TCAC beads was analyzed by the Thermo UltraDry™ energy dispersive spectrometer (EDS).

RESULTS AND DISCUSSION

Sorbent Screening and Characterization

According to the research study of Mi and co-workers,[11] protonated amino group on chitosan reacted more easily with $P_3O_{10}^{5-}$ at low pH of TPP solution. In another word, gel beads prepared in acidic TPP solution have a higher degree of ionic crosslinking. Therefore, in this study, pH 8.6 of TPP solution was selected to control the degree of crosslinking of chitosan. Table I summarizes the performances of TCAC and TCC beads prepared under different conditions for the adsorption of Ag (I) and Cu (II) from monometallic and bimetallic solutions. Results indicate that alkalization before crosslinking helps to obtain chitosan gel beads with higher total uptake capacity, and TCAC beads provided much more binding sites for Ag (I) than TCC beads. It is clearly that beads with lower degree of crosslinking (TCAC) are favorable to Ag (I) binding, whereas beads with higher degree of crosslinking (TCC) tend to bind more Cu (II). This reveals the adsorption of Ag (I) and Cu (II) take place at different sorption sites and amine group on chitosan is more selective to Ag (I).

As illustrated in Table I, concentration of STPP solution does not have significant influence on the sorbent performance. Therefore, TCAC beads prepared by crosslinking with 5.0% (w/v) STPP solution were selected for the remaining isotherm and kinetic studies.

To investigate the degree of ionic crosslinking between chitosan and TPP, FTIR analyses of chitosan powder, TCC, and TCAC beads were conducted and their spectra were compared in Figure 1. The characteristic IR peaks of chitosan powder are: band around 3273m cm^{-1} corresponding to —NH and —OH stretching vibration; 1650 cm^{-1} due to —NH deformation vibration; 1150 cm^{-1} for —CN stretching vibration and 1068 cm^{-1} due to

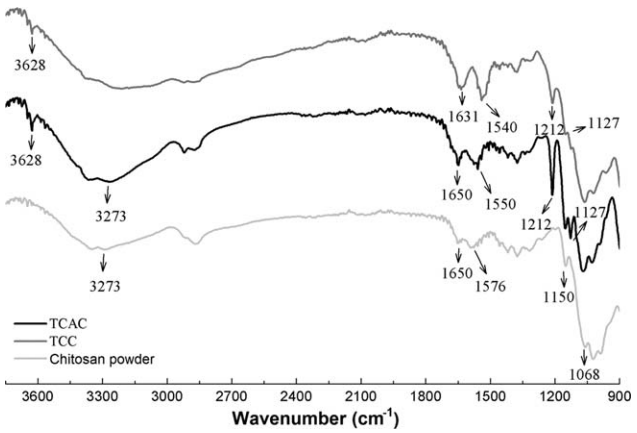

Figure 1. IR spectra of chitosan powder, TCC, and TCAC beads.

stretching vibration of —C—OH. Structure changes of TCC and TCAC beads due to ionic crosslinking were confirmed from their IR spectra. Band peak at 3628 cm^{-1} in the spectra of TCC and TCAC beads becomes clearly visible owing to —NH group in chitosan being broadened by the physical interactions with TPP,[24] indicating that crosslinking of TPP and chitosan took place on the amino groups. The shifts of amine peaks at 1650 and 1576 cm^{-1} on TCC and TCAC indicate the ionic interaction between the positively charged amino groups of chitosan and the negatively charged triphosphate groups.[25,26] The more remarkable band shift of amine group on the spectrum of TCC manifests the higher degree of crosslinking of TCC beads. In addition, a broad peak at 3550–3230 cm^{-1} on the IR spectrum of TCAC beads is assigned to the intermolecular hydrogen-bonded O—H from alkalization, which overlaps the peak of —NH. Sharp peaks at 1212 cm^{-1} and 1127 cm^{-1} on the spectra of TCC and TCAC beads are attributed to vibrations of —P═O bond of the TPP added,[20] indicating the successfully crosslinking of TPP on chitosan.

Swelling Properties

Swelling ability of TCC and TCAC beads in 5.0 vol % HNO_3, DI water and 0.1 M NaOH solution were carried out at room temperature. The swelling percentages of TCC beads in nitric acid, DI water, and NaOH solution were 65.0, 27.0, and 24.0%, respectively. The swelling ability of TCAC beads is much higher, being 135.0 and 126.0% in DI water and 0.1 M NaOH solution. Nevertheless, in 5.0 vol % HNO_3, TCAC beads swelled quickly and gradually dissolved within 12.0 h, indicating the weak chemical resistance of TCAC in acidic environment. At low pH, the swelling of the TCC and TCAC beads was mainly attributed to the scission of ionic-crosslinked chain. With the increase of pH of dissolution medium, the ionic-crosslinked chain of the beads didn not dissociate and the swelling percentages were getting smaller, so the swelling of TPP-crosslinked chitosan beads in high pH media would be mainly attributed to the hydration or ionization of unbound —NH_2 sites in chitosan.

Adsorption Kinetics

The adsorption kinetic data of Ag (I) and Cu (II) by TCAC beads was shown in Figure 2. Although TCAC beads has lower uptake capacity of Cu (II) than Ag (I), the adsorption of Cu (II) is faster than that of Ag (I). TCAC binding of Cu (II) was very fast during the first 4.0 h and the equilibrium was attained within 8.0 h, whereas the uptake of Ag (I) on TCAC beads kept on increasing and adsorption equilibrium was not completely arrived after 48.0 h of adsorption. The different sorption kinetics of Ag (I) and Cu (II) on the TCAC beads indicate that the Ag (I) sorption mechanism is different to that of Cu (II) on the binding sites of the beads. In addition, the gradual kinetics of Ag (I) sorption might be a big hurdle in the practical applications of TCAC beads.

Several adsorption kinetic models have been applied to interpret the adsorption kinetics and the rate limiting step during adsorption. The pseudo-first and -second order equations are mainly applied in the biosorption with sharing or exchange of electrons between functional groups and metal ions.[27,28] The intra-particle diffusion model which highlights the importance of mass transfer in the hydrogel beads has also been successfully applied to describe the sorption kinetics of metal ions.[12] In addition, Elovich equation[29] which assumes the adsorption occurred on the heterogeneous surface usually provides accurate explanations of the slow biosorption kinetics. In the current study, all the aforementioned rate equations were used to quantify the time effect on the uptake of Ag (I) and Cu (II) by the TCAC beads. The rate equations of the four different models are listed below.

Pseudo-first order equation:

$$q_{i,t} = q_{i,e}(1 - \exp(-k_{1,i}t)) \tag{5}$$

Pseudo-second order equation:

$$q_{i,t} = \frac{k_{2,i}q_{i,e}^2 t}{1 + k_{2,i}q_{i,e}t} \tag{6}$$

The intra-particle diffusion model:

$$q_{i,t} = k_{m,i}t^{1/2} \tag{7}$$

And the Elovich rate equation:

$$q_{i,t} = (1/\beta_i)\ln(\alpha_i\beta_i) + (1/\beta_i)\ln t \tag{8}$$

where $q_{i,e}$ nd $q_{i,t}$ (mg g^{-1}) are the amounts of metal ions i adsorbed onto TCAC at equilibrium and at time t, respectively, and $k_{1,i}$ (h^{-1}) is the rate constant of pseudo-first order kinetic model; $k_{2,i}$ (g mg^{-1} h^{-1}) is the rate constant of second-order kinetic model; $k_{m,i}$ (mg g^{-1} $h^{-0.5}$) is the intra-particle diffusion constant; while α_i (mg g^{-1} h^{-1}), and β_i (g mg^{-1} $(lnh)^{-1}$) are the initial adsorption and desorption rate constants for Elovich rate equation, respectively.

The kinetic parameters for the different rate equations were determined by linear and nonlinear curve fittings using MATLAB and the results are summarized in Table II. The measured kinetic data and the model predicted kinetic results are compared and illustrated in Figure 2(a–d). It was found that except for intra-particle diffusion model, all the other rate equations can provide very accurate predictions on the adsorption kinetics of Cu (II). For the adsorption of Ag (I), pseudo-second order and Elovich rate equations are better than pseudo-first and intrparticle diffusion models.

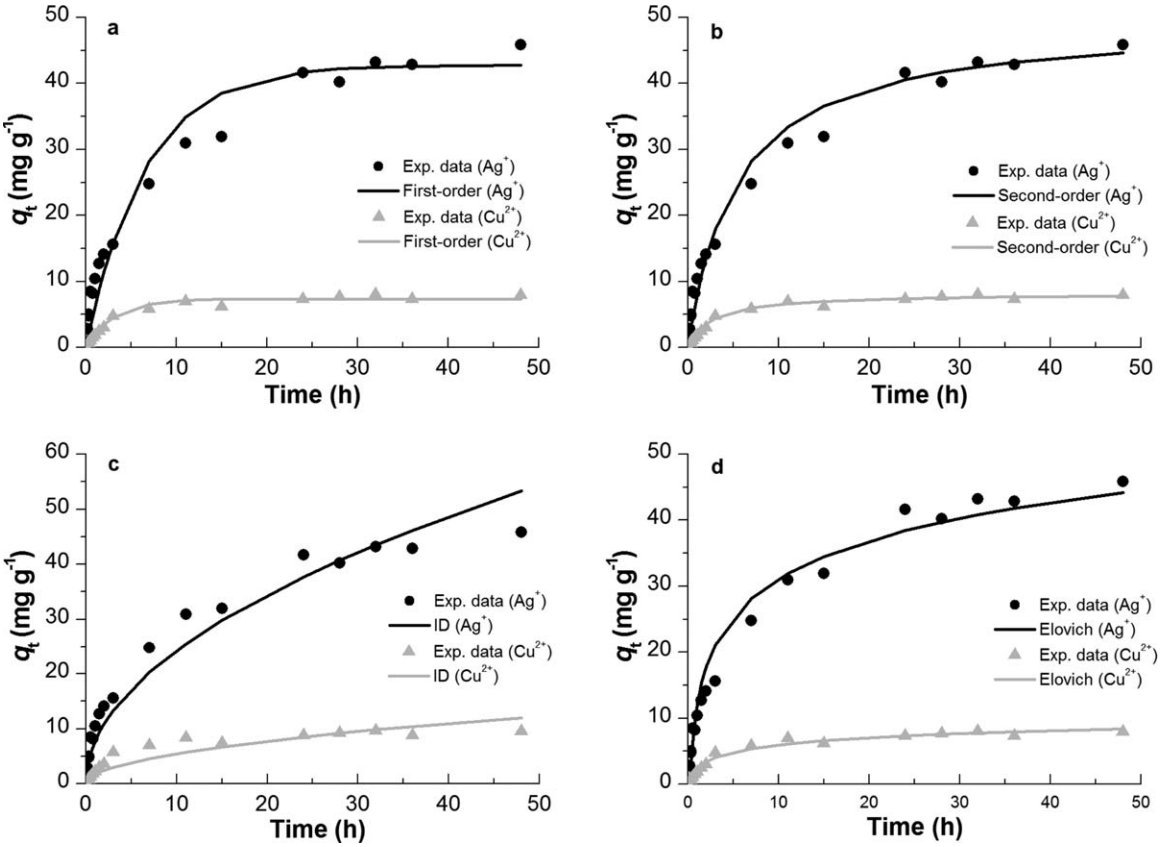

Figure 2. Comparison of different kinetic models for the sorption of Ag (I) and Cu (II) by TCAC beads.

Adsorption Isotherm

Adsorption isotherm illustrates the equilibrium characteristics of the competitive adsorption of Ag (I) and Cu (II) onto the TCAC beads. Sorption equilibrium results shown in Figure 3 confirm that TCAC beads have good selectivity toward Ag (I) as the uptake capacity of Ag (I) is much higher than that of Cu (II) from bimetallic solutions. The equilibrium uptake capacities of Ag (I) and Cu (II) both increase with the increase of concentration of metallic solutions. The relationship between adsorption capacity and equilibrium concentration of metal ions in the solution can be better described by isotherm models.

Langmuir and Freundlich isotherm models[30] were used in this study to explicate the adsorption equilibrium of Ag (I) and Cu (II) on TCAC beads. The Langmuir and Freundlich equations are given in eqs. (9) and (10), respectively,

Table II. Kinetic Parameters for Ag (I) and Cu (II) Adsorption on TCAC

		Rate parameters	
Kinetic equation		Ag (I)	Cu (II)
Pseudo-first order			
k_1	h^{-1}	0.154	0.319
q_e	mg g^{-1}	42.77	7.35
R^2		0.96	0.98
Pseudo-second order			
k_2	g mg^{-1} h^{-1}	3.8×10^{-3}	0.046
q_e	mg g^{-1}	49.57	8.22
R^2		0.98	0.98
Intra-particle diffusion			
k_m	g mg^{-1} $h^{-0.5}$	7.69	1.44
R^2		0.95	0.88
Elovich			
α	mg g^{-1} h^{-1}	34.98	6.66
β	g mg^{-1} $(lnh)^{-1}$	0.12	0.63
R^2		0.97	0.98

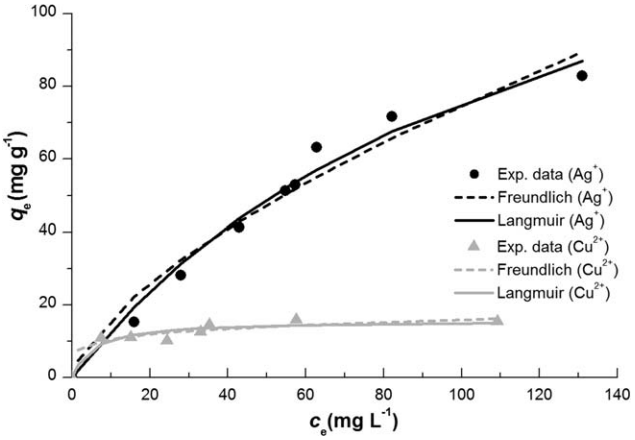

Figure 3. Non-linear adsorption isotherm of Ag (I) and Cu (II).

Table III. Isotherm Parameters of the Adsorption of Ag (I) and Cu (II) on TCAC Beads at T=25°C

	Langmuir			Freundlich		
Metal	b (L mg^{-1})	q_s (mg g^{-1})	R^2	K_F	n	R^2
Ag (I)	0.008	167.98	0.98	3.57	1.51	0.94
Cu (II)	0.188	15.73	0.95	7.02	5.65	0.96

$$q_i^* = \frac{q_{s,i} b_i c_{i,e}}{1 + b_i c_{i,e}} \quad (9)$$

$$q_i^* = K_{F,i} c_{i,e}^{1/n_i} \quad (10)$$

where q_i^* (mg g^{-1}) is the amount of metal ions i adsorbed per unit mass of adsorbent at equilibrium, $c_{i,e}$ (mg L^{-1}) is the equilibrium concentrations of remaining metal ions i in the solution, $q_{s,i}$ (mg g^{-1}) is the maximum biosorption capacity, b_i is the sorption equilibrium constant, $K_{F,i}$ is a constant indicative of the adsorption capacity of the sorbent, and $1/n_i$ is a measure of adsorption intensity.

The isotherm parameters of Langmuir and Freundlich models listed in Table III were determined by linear regression using MATLAB. Both models provide accurate sorption equilibria of Ag (I) and Cu (II) well in agreement with the measured data as demonstrated in Figure 3. Results from Table III and Figure 3 indicate that Langmuir isotherm delineates the experimental data slightly better than Freundlich.

Sorption Mechanism

The potential binding sites on the surfaces of TCAC available for the adsorption of Ag (I) and Cu (II) are presented in Figure 4. Because alkalization before crosslinking protects some amino groups from crosslinking, free amine groups on TCAC surfaces provide binding sites for both metal ions. It was reported that Cu (II) is usually bound with amine groups of chitosan via inter- or intramolecular complexation.[21,31] Due to the relative long chain of TPP, it is difficult for Cu (II) to be bound to TCAC surfaces through bridge model.[31] In addition, Cu (II) is more electropositive than Ag (I) and more electro donor atoms need to be involved in binding Cu (II), making Cu (II) inferior to Ag (I) in competing for binding sites. On the contrary, Ag (I) can easily bind to TCAC surfaces through the free amine and/or the vicinal hydroxyl groups.

To further explore the competitive adsorption mechanism of Ag (I) and Cu (II) on TCAC beads, IR spectra of the TCAC beads before and after monometallic/bimetallic adsorption as shown in

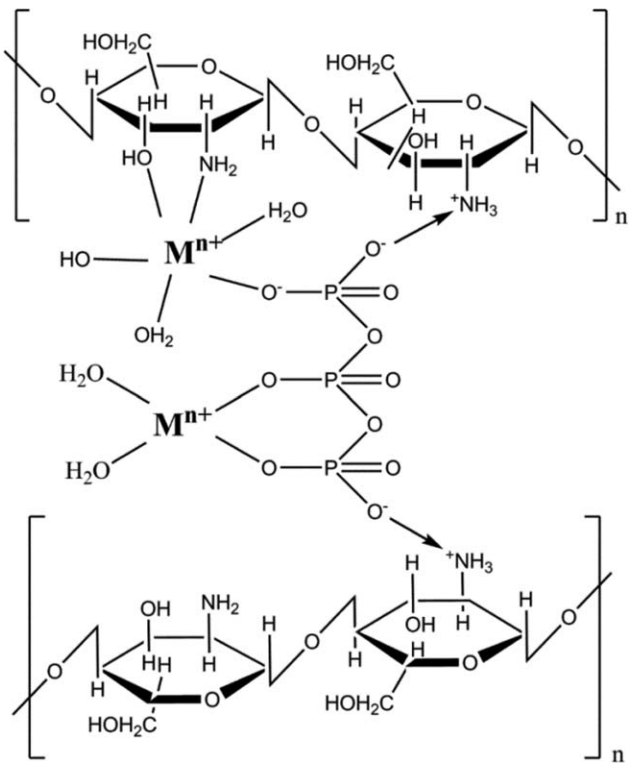

Figure 4. Possible binding sites on TCAC surfaces.

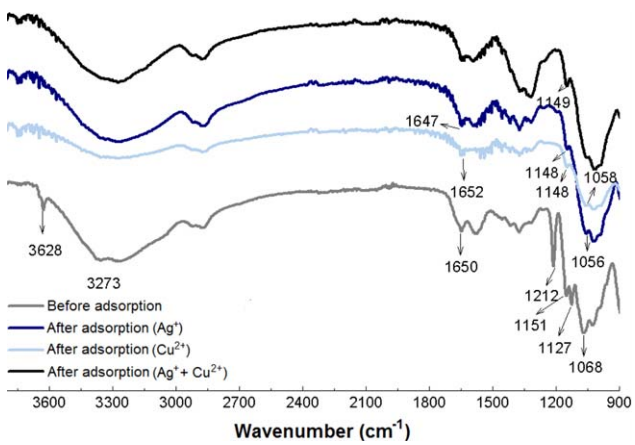

Figure 5. IR spectra of TCAC beads before and after metal uptake from different solutions. [Color figure can be viewed in the online issue, which is available at wileyonlinelibrary.com.]

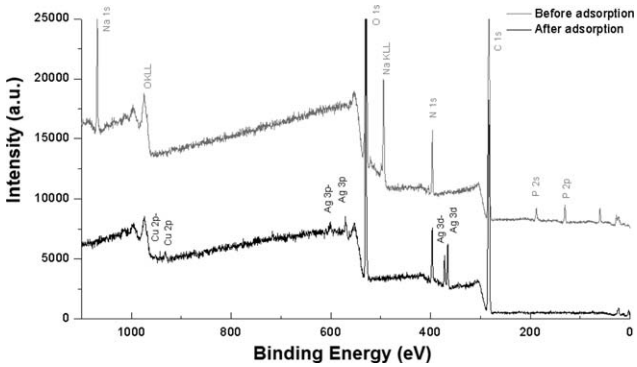

Figure 6. XPS survey spectra of TCAC beads before and after metal sorption.

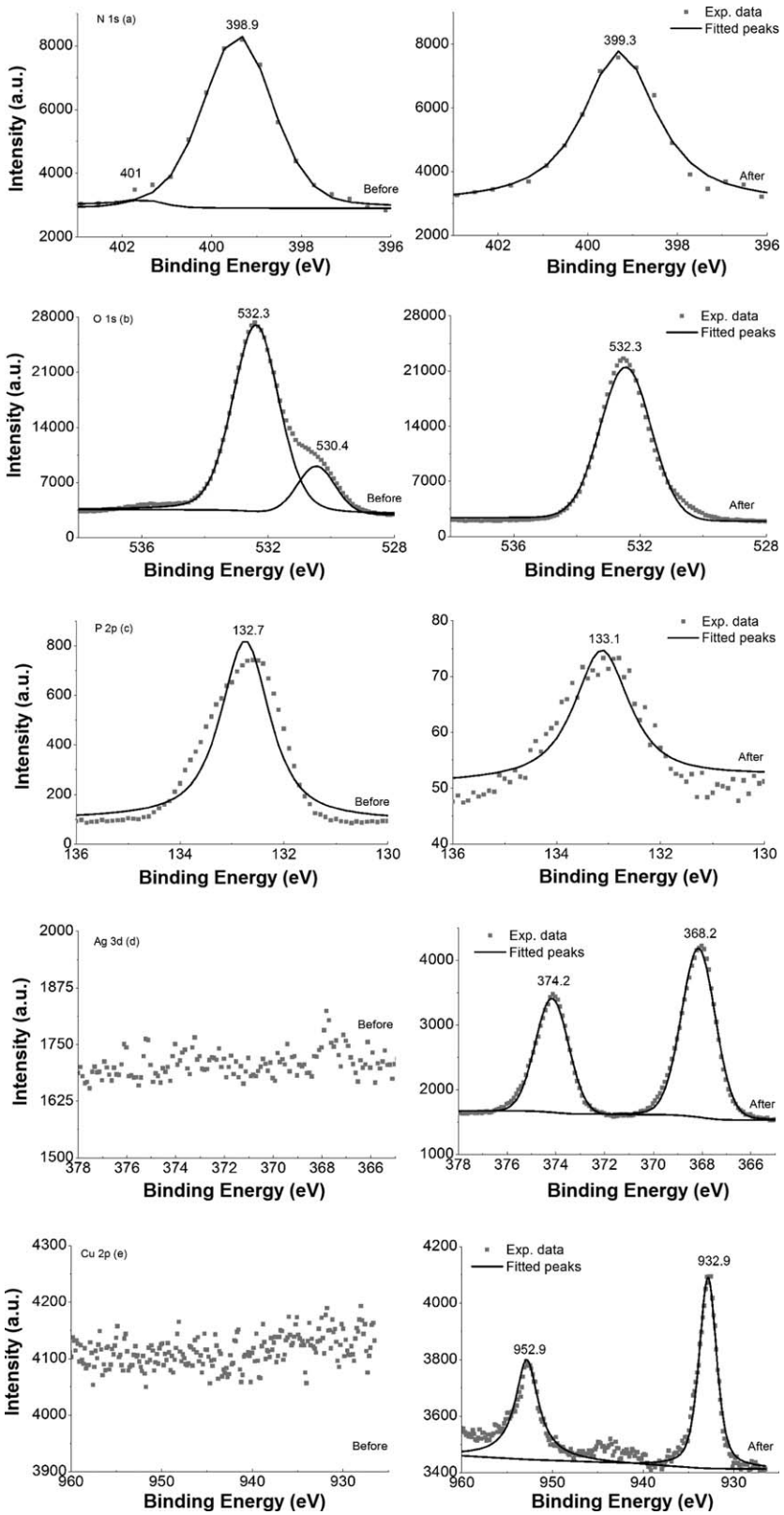

Figure 7. Fitted high-resolution photoemission spectra of N 1s (a), O 1s (b), P 2p (c), Ag 3d (d), and Cu 2p (e) before and after metal uptake for TCAC beads.

Figure 5 were studied. The peak shift at 3628 cm^{-1} after metal sorption in Figure 5 indicates that the amine group is involved in the adsorption of metal ions. The significant peak shift at 1068 cm^{-1} to 1058cm^{-1} after Cu (II) adsorption and to 1056 cm^{-1} after Ag (I) adsorption, confirms that —C—OH group contribute to the uptake of metal ions. The shifts at peak

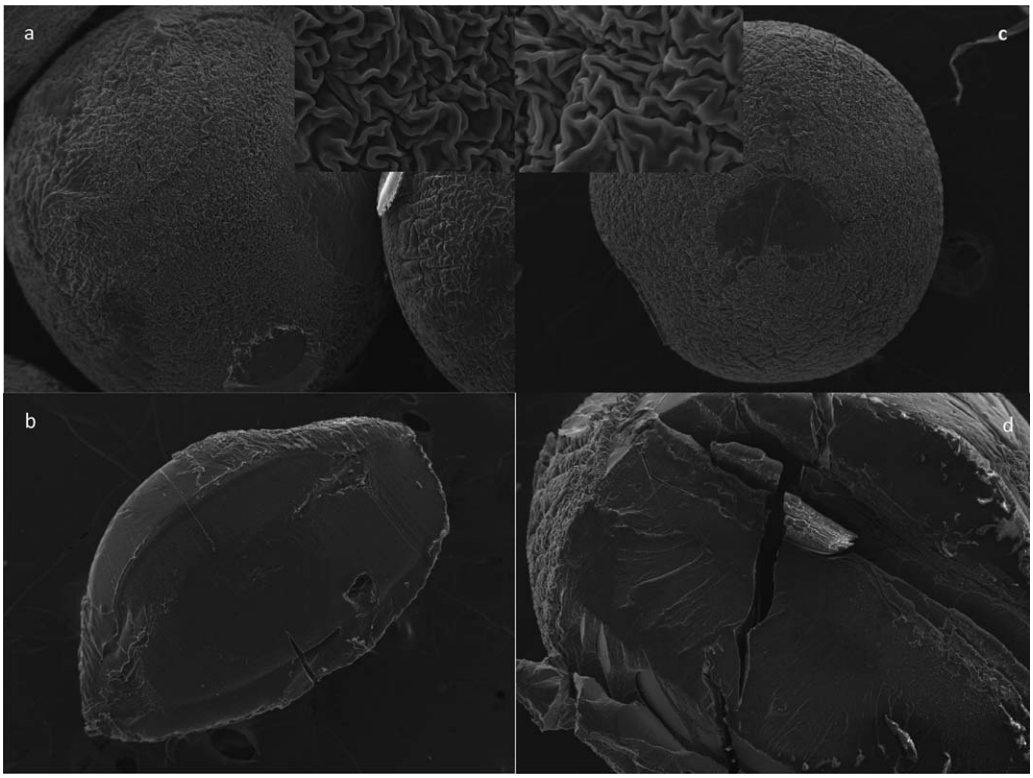

Figure 8. SEM images of the surface and cross-section morphologies of TCAC beads before (a & b) and after (c & d) metal uptake.

1650 cm^{-1} to higher wavenumber (1652 cm^{-1}) after Cu (II) uptake and lower wavenumber (1647 cm^{-1}) after Ag (I) uptake prove the involvement of —NH_2 groups in metal uptake. Moreover, IR spectrum after bimetallic adsorption shows very similar peak shift at 1650 cm^{-1} to the one with single Ag (I) sorption, suggesting that the adsorption of Ag (I) by TCAC is dominant during bimetallic adsorption. The sharp peaks at 1127 and 1212 cm^{-1} arising from the —P═O stretching vibration, disappeared after adsorption, which reflects the interaction between Ag (I)/Cu (II) and $^{-}$O—P═O.

XPS spectra have widely been used to identify the existence of a particular element and to distinguish the different forms of the same element in a material. Figure 6 illustrates the survey spectra of TCAC beads before and after metal adsorption. From the survey spectrum of TCAC beads before metal uptake, the binding energy (BE) peaks at 284.8 eV for C 1s, 532.3 eV for O 1s and 398.9 eV for N 1s are clearly visible. Na 1s peak with BE at 1071.0 eV and two BE peaks at 190.2 and 132.7 eV for P 2s and P 2p proved the successful crosslinking of STPP on chitosan surfaces. The binding of Ag (I) and Cu (II) on TCAC surfaces was verified from the photoemission bands Ag $3d_{3/2}$, Ag $3d_{5/2}$, Cu $2p_{1/2}$ and Cu $2p_{3/2}$ on the XPS spectrum of TCAC after sorption.

High resolution XPS spectra of N 1s, O 1s and P 2p as well as their deconvoluted fitted curves are demonstrated in Figure 7(a–c) for TCAC beads before and after metal uptake. BE peaks at 398.9 and 401.0 eV are visible for N 1s spectrum before sorption. N 1s peak at 398.9 eV was assigned to free amine group (—NH_2) whereas the higher BE peak at 401.0 eV was assigned to the protonated amine group (—NH_3^+) presented on TCAC surfaces.[32] After metal adsorption, N 1s peak at 398.9 eV shifted to 399.3 eV, suggesting electron from nitrogen was shared with metal ions and hence the electron cloud density of nitrogen was reduced, resulting in a slightly higher BE peak. N1s peak at 401.0 eV corresponding to protonated amine shifted to lower binding energy after sorption, suggesting a possible binding of protonated amine with metal anions.[33]

The XPS data of O 1s on TCAC before and after Ag (I) and Cu (II) adsorption are shown in Figure 7(b). The peaks with BE at 532.3 and 530.4 eV are assigned to organic oxygen in chitosan chain and inorganic oxygen in $P_3O_{10}^{5-}$ group.[34] The decrease in the intensity of O 1s peak at 532.3 eV after adsorption indicates that Ag (I) or Cu (II) adsorption took place on —C—OH. Moreover, the peak at 530.4 eV shifted to higher BE on the O 1s spectrum after adsorption, indicating the decrease of electron density of oxygen. In this case, oxygen acts as the electron donor when binding with metal ions.

Figure 7(c) shows the P 2p spectra of TCAC and the fitted curves. BE at 132.7 eV, which is assigned to $P_3O_{10}^{5-}$ group shifted to 133.1 eV after adsorption, proving the involvement of $P_3O_{10}^{5-}$ group in metal binding. In addition, the low signal intensity of P 2p, especially after adsorption, revealed that the crosslinking density of TCAC beads is low. The dramatic decrease of the signal intensity of P 2p after adsorption stemmed from the increased amount of Ag (I) and Cu (II) on TCAC surface, leading to a decrease of weight percentage of P on the sorbent surface.

Table IV. Desorption of Ag (I) and Cu (II) from Metal Loaded TCAC Beads

Metal	Desorbent and initial pH	Initial metal uptake (mg/g)	Desorption ratio (%) and solution pH value at different time		
			2.5 h	8.0 h	24.0 h
Ag (I)	0.1 M $Na_2S_2O_3$ (pH 6.1)	51.25	96% (pH 7.8)	96% (pH 7.8)	96% (pH 7.8)
	0.1 M $Na_2S_2O_3$ & 0.01M EDTA (pH 5.8)	51.25	100% (pH 7.8)	100% (pH 7.8)	100% (pH 7.8)
	0.01 M EDTA (pH = 4.7)	51.25	8% (pH5.6)	8% (pH 5.8)	8% (pH 6.1)
	0.01 M EDTA & 0.1 M H_2SO_4 (pH = 3)	51.25	53% (pH 3.4)	72% (pH 3.5)	96% (pH 3.76)
Cu (II)	0.1 M $Na_2S_2O_3$ (pH 6.1)	14.49	58% (pH 7.8)	77% (pH 7.8)	95% (pH 7.8)
	0.1 M $Na_2S_2O_3$ & 0.01M EDTA (pH 5.8)	14.49	98% (pH7.8)	99% (pH7.8)	99% (pH7.8)
	0.01 M EDTA (pH = 4.7)	14.49	99% (pH5.6)	99% (pH 5.8)	99% (pH 6.1)
	0.01M EDTA & 0.1 M H_2SO_4 (pH = 3)	14.49	97% (pH 3.4)	97% (pH 3.5)	97% (pH 3.76)

Ag binding energies in TCAC beads after metal uptake were found to be at 374.2 and 368.2 eV as illustrated in Figure 7(d). The binding energy of $Ag3d_{5/2}$ is most commonly used to determine the chemical state of Ag. However, silver is an element that is rather difficult to assess from its XPS peaks due to very small chemical shifts. The BE of Ag $3d_{5/2}$ in Figure 7(d) can be assigned to metal silver, Ag_2O or silver complexes.[35,36] The powder X-ray diffraction (XRD) results of the Ag(I) loaded TCAC beads exclude the existence of metal silver and Ag_2O. Thereby, the BE of $Ag3d_{5/2}$ is attributed to compounds formed between Ag (I) and —O—R in this study.[36] Cu $2p_{1/2}$ and Cu $2p_{3/2}$ can also be observed from the XPS spectrum of TCAC after sorption shown in Figure 7(e). Cu $2p_{1/2}$ peak at 952.9 eV and Cu $2p_{3/2}$ peak at 932.9 eV are corresponding to an oxidation state (Cu^{2+}) of copper,[34] suggesting the binding of Cu (II) with oxygen in the $^-$O—P═O group.

Results from IR and XPS analyses of TCAC beads clearly revealed that amine, hydroxyl and $P_3O_{10}^{5-}$ groups are the main binding sites for Ag (I) and Cu (II) with amine and hydroxyl groups more selective to Ag (I) and $P_3O_{10}^{5-}$ group more selective to Cu (II). To confirm the inexistence of metal ion reduction during the biosorption process, outer surface and cross-section of the TCAC beads before and after metal uptake were examined by SEM. The surface and cross-section morphologies of TCAC beads are illustrated in Figure 8. Smooth and homogeneous structure was observed for sorbents before and after metal uptake. There was no indication of the formation of metal silver, metal copper and other precipitates even though an average of 21.57 w % of Ag (I) and 3.48 w % of Cu (II) was detected on the cross-section of metal ion loaded TCAC beads by EDS.

Desorption of Metal Ions

In this study dilute sulfuric acid, sodium thiosulfate and EDTA solutions were applied to desorb Ag (I) and Cu (II) from loaded TCAC sorbents to evaluate their desorption efficiency. As shown in Table IV, 0.1 M $Na_2S_2O_3$ can desorb both Ag (I) and Cu (II) but with different desorption rates, while EDTA can only desorb Cu (II) although the desoporption rate of Cu (II) is quite fast. As a result, when aqueous solution containing 0.1 M $Na_2S_2O_3$ and 0.01M EDTA was used as the desorbent, both Ag (I) and Cu (II) can be completely desorbed from the loaded TCAC beads in 2.5 h. Eluent containing 0.1 M H_2SO_4 and 0.01 M EDTA is also capable of completely desorbing the two metal ions, but very slow in desorbing Ag (I). The increase of solution pH after desorption is proportional to the increase of desorption ratio, proving the correctness of the measured desorption ratio.

CONCLUSION

A modified chitosan sorbent was synthesized in this study by alkalizing chitosan, followed by crosslinking with TPP and was used for the competitive adsorption of Ag (I) and Cu (II) from bimetallic solutions. The newly synthesized beads have very high uptake capacity and very good selectivity toward Ag (I). The highest uptake capacities of Ag (I) and Cu (II) were found to be 82.9 and 15.5 mg/g, respectively, at 25°C with an initial concentration of each metal being 2.0 m*M* and the sorbent dosage of 1.0 g L^{-1}. The Langmuir isotherm can describe the adsorption isotherm of Ag (I) and Cu (II) on TCAC very well. Experimental results indicate that sorption of Cu (II) is faster than the uptake of Ag (I) by the synthesized beads. Eluent containing 0.1 M $Na_2S_2O_3$ and 0.01 M EDTA is very efficient in regenerating the metal loaded beads. Results from FTIR and XPS analyses of the chitosan gel beads before and after metal sorption revealed that amine, hydroxyl and $P_3O_{10}^{5-}$ groups are the main binding sites for Ag (I) and Cu (II) with amine and hydroxyl groups more selective to Ag (I).

ACKNOWLEDGMENTS

Support of this research from RDC Ignite Grant and Memorial University of Newfoundland are gratefully acknowledged. The authors would also like to thank Dr. Wanda Aylward for helpful suggestions and discussions on the XRD and SEM/EDS measurements of the prepared biosorbent.

REFERENCES

1. Park, S. I.; Kwak, I. S.; Won, S. W.; Yun, Y.-S. *J. Hazard. Mater.* **2013**, *248*, 211.
2. Guibal, E. *Sep. Purif. Technol.* **2004**, *38*, 43.
3. Niu, H.; Voleskey, B. *Hydrometallurgy* **2006**, *84*, 28.

4. Li, C.; Hein, S.; Wang, K. *Mater. Sci. Technol.* **2008**, *24*, 1088.
5. Wan Ngah, W. S.; Fatinathan, S. *Chem. Eng. J.* **2008**, *143*, 62.
6. Zhao, J.; Zhu, Y. J.; Wu, J.; Zheng, J. Q.; Zhao, X. Y.; Lu, B. Q.; Chen, F. *J. Colloid Interf. Sci.* **2014**, *418*, 208.
7. Kumar, G.; Smith, P. J.; Payne, G. F. *Biotechnol. Bioeng.* **1999**, *63*, 154.
8. Miretzky, P.; Cirelli, A. F. *J. Hazard. Mater.* **2009**, *167*, 10.
9. Sureshkumar, M.; Das, D.; Mallia, M.; Gupta, P. *J. Hazard. Mater.* **2010**, *184*, 65.
10. Mi, F. L.; Shyu, S. S.; Lee, S. T.; Wong, T. B. *J. Polym. Sci. Phys.* **1999**, *37*, 1551.
11. Mi, F. L.; Sung, H. W.; Shyu, S. S.; Su, C. C.; Peng, C. K. *Polymer* **2003**, *44*, 6521.
12. Wan Ngah, W. S.; Fatinathan, S. *J. Environ. Manage.* **2010**, *91*, 958.
13. Wu, S.-J.; Liou, T.-H.; Yeh, C.-H.; Mi, F.-L.; Lin, T.-K. *J. Appl. Polym. Sci.* **2013**, *127*, 4573.
14. Volesky, B. *Water Res.* **2007**, *41*, 4017.
15. Kotrba, P. In Microbial Biosorption of Metals, Kotrba, P.; Mackova, M.; Macek, T. Eds.; Springer: New York, **2011**.
16. Won, S. W.; Kotte, P.; Wei, W.; Lim, A.; Yun, Y.-S. *Bioresource Technol.* **2014**, *160*, 203.
17. Donia, A. M.; Atia, A. A.; Elwakeel, A. K. Z. *Hydrometallurgy* **2007**, *87*, 197.
18. Guzman, J.; Saucedo, I.; Revilla, J.; Navarro, R.; Guibal, E. *Int. J. Biol. Macromol.* **2003**, *33*, 57.
19. Osunlaja, A. A.; Ndah, N. P.; Ameh, J. A. *Afr. J. Biotechnol.* **2009**, *8*, 4.
20. Guibal, E.; Vincent, T.; Navarro, R. *J. Mater. Sci.* **2014**, *49*, 5505.
21. Rhazi, M.; Desbrières, J.; Tolaimate, A.; Rinaudo, M.; Vettero, P.; Alagui, A. *Polymer* **2002**, *43*, 1267.
22. Messler, R. W. The Essence of Materials for Engineers; Jones & Bartlett publishers: Sudbury, MA., **2010**; p 32.
23. Butterman, W. C.; Hilliard, H. E. Silver, Open-File Report 2004-1251. U.S. Geological Survey, **2005**.
24. Ibezim, E. C.; Andrade, C. T.; Marcia, C.; Barretto, B.; Odimegwu, D. C.; De Lima, F. F. *Ibnosina J. Med. BS* **2011**, *3*, 77.
25. Lee, S. T.; Mi, F. L.; Shen, Y. J.; Shyu, S. S. *Polymer* **2001**, *42*, 1879.
26. de Moura, M. R.; Aouada, F. A.; Avena-Bustillos, R. J.; McHugh, T. H.; Krochta, J. M.; Mattoso, L. H. C. *J. Food Eng.* **2009**, *92*, 448.
27. Yuh-Shan, H. *Scientometrics* **2004**, *59*, 171.
28. Ho, Y.-S. *J. Hazard. Mater.* **2006**, *136*, 681.
29. Chien, S.; Clayton, W. *Soil Sci. Soc. Am. J.* **1980**, *44*, 265.
30. LeVan, M. D.; Vermeulen, T. *J. Phys. Chem.-US* **1981**, *85*, 3247.
31. Lü, R.; Cao, Z.; Shen, G. *J. Mol. Struc.-Theochem* **2008**, *860*, 80.
32. Boufi, S.; Vilar, M. R.; Ferraria, A. M.; Botelho do Rego, A. M. *Colloid. Surf. A* **2013**, *439*, 151.
33. Mack, C.; Wilhelmi, B.; Duncan, J.; Burgess, J. *Biotechnol. Adv.* **2007**, *25*, 264.
34. Vieira, R. S.; Oliveira, M. L. M.; Guibal, E.; Rodríguez-Castellón, E.; Beppu, M. M. *Colloid. Surf. A* **2011**, *374*, 108.
35. Moulder, J. F.; Stickle, W. F.; Sobol, P. E.; Bomben, K. D. Handbook of X-ray Photoelectron Spectroscopy; Perkin Elmer Eden Prairie: MN, **1992**; Vol. *40*.
36. Gerenser, L. J. J. *Vac. Sci. Technol. A* **1990**, *8*, 3682.